Wood Science and Technology
https://doi.org/10.1007/s00226-023-01518-x

ORIGINAL

Bark-based biorefineries: anatomical and chemical characterization of the bark of endemic *Quercus vulcanica* of Turkey

Ali Umut Şen[1] · Rita Simões[1] · Cengiz Yücedağ[2] · Teresa Quilhó[1] · Vicelina Sousa[1] · Isabel Miranda[1] · Ângela Fernandes[3,4] · Helena Pereira[1]

Received: 18 September 2023 / Accepted: 27 November 2023

Abstract

The detailed anatomical and chemical features of the bark from endemic *Quercus vulcanica* in Turkey are reported here for the first time and discussed in the perspective of integration into a bark-based biorefinery system. The bark of *Q. vulcanica* trees was collected and studied through observations using light and scanning electron microscopy, wet-chemical analysis, inorganic elemental and FTIR analyses, GC–MS determinations of lipophilic extractives and suberin monomers, as well as TBARS antioxidant activity of hydroethanolic extracts. The bark of *Q. vulcanica* comprises phloem and a rhytidome with thin periderms and a few cork layers. The ash content is high (16.4%), primarily consisting of calcium oxalate crystals. Extractives were present in a high amount (23.1%) of which 88% corresponded to hydrophilic extractives (10.3% ethanol, and 10.1% water solubles). The suberin content is low (3.7%), which aligns with the small proportion of cork in the bark rhytidome. The composition of suberin is characterized by similar proportions of α, ω-alkanoic diacids and ω-hydroxyalkanoic acids, with 18-hydroxy-9-octadecenoic acid (26% of monomers) and octadec-9-enedioic acid (20.6%) as the main monomers. The lignin content is 21.9%, and the monomeric composition of polysaccharides includes glucose, xylose, arabinose, galactose, rhamnose, and acetyl groups. The lipophilic extractives are mainly composed of terpenoids (72.2% of all compounds), with friedelin and friedelanol as the main compounds. Hydroethanolic extracts, obtained under mild conditions with a yield of 10.2%, exhibited antioxidant activity (TBARS assay, EC_{50} value of 55 µg/mL). The overall chemical and structural properties of *Q. vulcanica* bark indicate promising potential for biorefineries.

Extended author information available on the last page of the article

Published online: 02 January 2024

Introduction

Oaks cover approximately one-third of Turkey's total forest area, with 18 species (Yaltirik 1984), including endemic species, such as *Quercus vulcanica* Boiss. ex Kotschy, *Q. macranthera* subsp. *syspirensis* (K. Koch) Menitsky (Yaltirik 1984), and *Q. trojana* subsp. *yaltirikii* Ziel., Petrova & D.Tomasz. (Zieliński et al. 2006). *Q. vulcanica*, also known as the volcanic oak or kasnak oak belongs to the white oaks group (family Fagaceae, genus *Quercus*, subgenus *Quercus*, section *Quercus*).

Q. vulcanica is a relict tree species (Atalay et al. 2014) that may reach a height of 25–30 m and a diameter of 1.6 m (Yaltirik 1984). Its distribution occurs at high altitudes between 1200 and 1800 m in the southwest to central-north of Anatolia (Yücedağ et al. 2021). Currently under protection by the national forest service, a pure forest of approximately 1300 ha of *Q. vulcanica* is located in the Kovada lake area of Isparta city, in western Turkey. The species is locally called kasnak meşesi (hoop-frame or rim oak) because its wood was possibly used as a frame for embroidery or sieves. The wood was particularly appreciated for the production of wood veneers due to its relatively narrow annual rings (Yaltirik 1984). Interestingly, the wood of *Q. vulcanica* was tested to produce oak barrels for aging cognac liquors as a substitute for France-imported *Q. petraea* wood, with positive results (Kayacık 1977). It was also tested for the aging of Turkish wines and rakı (Kayacık 1977). However, these tests were discontinued, and no commercial barrel production from *Q. vulcanica* wood has been reported.

It is well recognized that protection of forest species is easier when integrated within a valorization program targeting economic and social benefits. Additionally, the circular economy approach is now increasingly accepted, advocating for the adoption of a full resource use philosophy that utilizes waste materials to produce materials, chemicals, and energy (Antoniou et al. 2019; Awasthi et al. 2020). Tree barks are one example since they are usually considered waste forest-based biomass materials, often downgraded due to the presence of metals or sand impurities, or by their higher ash and lower polysaccharide content, as well as lower mechanical properties as compared to wood (Fengel and Wegener 1984). Thus, barks are usually left in the forest or kept on the logs until processing when they are removed and subsequently burned with a very low added value. Recently tree barks have been put forward as biomass resources for biorefineries, drawing attention to their interesting chemical and structural features and highlighting their potential contribution to the overall forest and biomass economy (Pasztory et al. 2016). Given the diversity of bark characteristics, the first step in developing the design of the best-suited conversion pathways is to conduct a detailed structural and chemical study.

The protection and valorization of *Q. vulcanica* will therefore require detailed information on the tree's biomass fractions, namely its bark. The current knowledge is scarce and particularly focused on the properties of wood, such as anatomy (Merev 1998), physical and mechanical properties (Göker et al. 2001), and chemical composition (Ucar et al. 1999). Only one study analyzed the

chemical composition of the bark, which reported that *Q. vulcanica* bark contains high amounts of ash and extractives, and palmitic acid (C16:0) and linoleic acid (C18:2), as well as friedelin and sitosterol, were identified in the lipophilic extractive fraction (Balaban and Uçar 2001). The chemical composition of ash, extractives, and suberin in *Q. vulcanica* bark is currently unknown, as well as its structural and anatomical description. However, these are important parameters for the design of bark-based biorefineries and, therefore, need to be characterized.

This study investigates in detail the *Q. vulcanica* bark to establish a first background knowledge to allow the selection of exploitation routes and contribute to establishing a circular economy with benefits for local populations and overall species protection. This study provides the first detailed characterization of *Q. vulcanica* bark, reporting its chemical composition and a qualitative description of its structure and anatomy. The bark of *Q. vulcanica* trees was collected and analyzed for chemical properties, including summative composition, elemental analysis, composition of lipophilic extractives and of suberin, as well as the characterization of surface functional groups. The bark anatomical features were also characterized in detail through microscopic observations.

Materials and methods

Sampling

Bark specimens from *Quercus vulcanica* trees were collected in the Isparta region of western Turkey, within the Kovada Lake National Park area (coordinates 37° 44′ 55″ N 30° 49′ 76″ E). The sampling location is situated at an altitude of 1500 m and exposed to an average annual temperature of 10.1 °C (Aslan and Ayvaz 2009). A total of five trees, averaging 40 years of age, were selected for the sampling following the TAPPI standard T 257 os-76. Bark fragments of approximately 20 cm × 20 cm × 2 cm were peeled from the tree trunks at a height of 1.30 m. For chemical analysis, the samples were triturated using a hammer mill (Retsch SK,) and the resulting granulated bark was sieved to retain fractions in the range of 40–60 mesh (250–420 µm) for subsequent analysis.

Anatomical characterization

The bark specimens were impregnated with DP1500 polyethylene glycol for light microscopy observations. Transverse and longitudinal microscopic sections, with a thickness of about 17 µm, were prepared using a Leica SM 2400 sliding microtome and an adhesive tape for sample retrieval. These sections were stained using a double staining with chrysodine and astra blue, and suberin was selectively stained using Sudan 4. The microscopic slides were then prepared for observation as detailed in Şen et al. (2011). The dissociated bark cells were also prepared for observation as previously described (Şen et al. 2011).

Microscopic analysis was conducted using a Nikon Microphot-FXA microscope connected to a digital camera (Nikon DS—Fi1c). Furthermore, the bark samples were also subjected to scanning electron microscopy (SEM) using a TM3030Plus Tabletop Microscope (Hitachi) operating at 5 kV, and digital images were recorded.

The terminology used for describing bark characteristics conformed to the IAWA List of Microscopic Bark Features (Angyalossy et al. 2016).

Summative chemical composition

The overall chemical composition, which comprises the contents of ash, extractives, suberin, lignin, and polysaccharides, was assessed on dry bark samples. The bark samples underwent overnight (16 h) drying at 60 °C followed by a subsequent drying at 100 °C for 2 h. The ash content was determined by incinerating approximately 2 g of bark in an oven at 550 °C overnight (for 16 ± 1 h). The total extractive content was determined via three consecutive Soxhlet extractions, following the procedure detailed in TAPPI Standards (T204 om-88 and T207 om-93). These extractions involved the use of dichloromethane (CH_2Cl_2-DCM), ethanol (C_2H_5OH-EtOH), and water (H_2O) as solvents, each extraction lasting for 6 h, 18 h, and 18 h, respectively.

Suberin content was determined by subjecting the previously extracted material to methanolysis. Approximately 1.5 g extractive-free sample was reacted with 100 mL of a 3% methanolic solution containing sodium methoxide for 3 h, followed by filtration and methanol washing. The residue was then refluxed with 100 mL of methanol for 15 min, followed by filtration. The filtrates were mixed, acidified to pH 6 using 2 M sulfuric acid, and evaporated to dryness. The resulting residue was suspended in 50 mL of water, and extracted using dichloromethane by applying three successive liquid–liquid extractions, each with 50 mL of dichloromethane. Later the extracts were dried using anhydrous sodium sulfate, and the solvent was evaporated to retain the concentrate for compositional analysis. The aqueous phase was preserved for glycerol analysis.

The Klason and acid-soluble lignin contents were determined in accordance with TAPPI T 222 om-88 and TAPPI UM 250 Standards, on previously extracted and desuberinised samples. This process involved reacting 72% H_2SO_4 (3.0 mL) with 0.35 g of the suberin-free material, by placing the mixture in a water bath at 30 °C for 1 h, diluting it to a 4% H_2SO_4 concentration, and then hydrolyzing it for 1 h at 120 °C (Sluiter et al. 2008).

The polysaccharide content was quantified by measuring the monosaccharide monomers released after the H_2SO_4 hydrolysis during the lignin determination. The sugar monomers were quantified using high-performance anion-exchange chromatography (HPAEC) with Aminotrap plus CarboPac SA10 anion exchange columns. All wet chemical experiments were performed with four repetitions.

Inorganic elemental composition

Phosphorus content was determined by spectrophotometric method by using a Hitachi U-2000 Vis/UV instrument, while the contents of Ca, Mg, Na, K, Cu, Mn,

Zn, S, Fe, and B were assessed using atomic absorption spectrophotometry with a Pye Unicam SP-9 apparatus (Cambridge, UK). This analysis was performed after a hydrochloric digestion of the ash.

FTIR analysis

The FTIR analysis was applied as a complementary method to wet chemical analysis and inorganic elemental analysis. Bark powder (particles under 180 µm) was oven-dried at 105 °C for 1 h before experimentation. Subsequently, the samples were placed on the diamond (ATR-FTIR), and reflectance spectra were obtained using a mid-infrared FTIR spectrometer (Perkin Elmer Spectrum Two), covering the range of 4000–400 cm^{-1} with a spectral resolution of 8 cm^{-1}. The spectra were normalized and baseline corrected before interpretation.

Composition of lipophilic extractives

The bark lipophilic extractives in dichloromethane (5 mL) were evaporated under a stream of nitrogen and subsequently dried at room temperature overnight under vacuum. The presence of esterified structures was assessed by dissolving 2 mg of the dichloromethane extracts in a 0.5 M sodium hydroxide solution in 50% aqueous methanol followed by heating at 100 °C, under a nitrogen atmosphere for approximately 60 min. Afterwards, the reaction mixture was cooled, acidified to pH 2 using 1 M hydrochloric acid, and extracted with dichloromethane three times. The solvent was evaporated to dryness. Prior to the GC–MS analysis, the lipophilic extracts were derivatized by dissolving in 100 µL of pyridine and adding 100 µL of bis(trimethylsily)-trifluoroacetamide (BSTFA). This derivatization process converted hydroxyl and carboxyl groups into trimethylsilyl (TMS) ethers and esters, respectively. The reaction mixture was kept at 60 °C for 30 min in an oven before the GC–MS analysis [EMIS, Agilent 5973 MSD, 70 eV, MS source 220 °C] under the following GC conditions: Zebron 7HGG015-02 Phenomenex column (30 m, 0.25 mm; ID, 0.1 µm film thickness), injector at 280 °C, and an oven temperature program starting at 100 °C (1 min), followed by a ramp to 150 °C (10 °C min^{-1}), 300 °C (4 °C min^{-1}), 370 °C (5 °C min^{-1}), and finally 380 °C (8 °C min^{-1}), with a holding time of 5 min. The lipophilic compounds were identified as TMS derivatives by comparing the mass spectra with those in a GC–MS spectral library (Wiley, NIST) and by analyzing the fragmentation patterns. The peak areas in the total ion chromatogram (TIC) were determined and expressed as normalized relative percentages. Triplicate injections were performed for each aliquot.

Composition of suberin

The monomeric composition of suberin was determined using aliquots obtained from the alcoholysis products extracted with dichloromethane after suberin depolymerization. These samples were evaporated and subjected to trimethysilyl derivatization before the immediate analysis by GC–MS. The GC–MS analysis

was conducted using a Zebron 7HGG015-02 column (Phenomenex, Torrance, CA, USA) (30 m, 0.25 mm; ID, 0.1 μm film thickness). The injector temperature was 400 °C and the oven temperature program started at 50 °C (held for 1 min), followed by a ramp of 10 °C min^{-1} to 150 °C, 5 °C min^{-1} to 200 °C, 4 °C min^{-1} to 300 °C, and 10 °C min^{-1} to 380 °C (held for 5 min). The mass spectrometer (MS) source was maintained at 220 °C, and the electron impact mass spectra (EIMS, 70 eV) were recorded.

The glycerol released during suberin depolymerization was quantified from the aqueous layer obtained after the liquid–liquid separation of the suberin depolymerization fraction using liquid chromatography (LC). The determination was carried out using a Dionex ICS-3000 system equipped with an electrochemical detector (Sunnyvale, CA, USA). The LC system employed Aminotrap plus CarboPac SA10 anion-exchange columns (Thermo Scientific, Waltham, MA, USA) and a mobile phase consisting of an aqueous 2-nM sodium hydroxide (NaOH) solution at a flow rate of 1.0 mL/min, all maintained at 25 °C.

Antioxidant properties of hydroethanolic extracts

The antioxidant activity of hydroethanolic extracts from the *Q. vulcanica* bark samples was assessed using a cell-based thiobarbituric acid reactive substances (TBARS) assay. Initially, granulated bark samples (~5 g, 250–420 μm) were stirred in 30 mL of an ethanol/water mixture (80:20, *v*/*v*) at 25 °C for 1 h and then filtered using a filter paper (Whatman No. 4). The residue underwent a second extraction with an additional 30 mL of the hydroethanolic mixture. The combined extracts were concentrated under reduced pressure using a Büchi R-210 rotary evaporator (Flawil, Switzerland) at 40 °C and subsequently lyophilized with a FreeZone 4.5 system (Labconco, Kansas City, MO, USA).

For the TBARS assay, the hydroethanolic extracts were dissolved in water and diluted, resulting in concentrations ranging from 10 to 0.3125 mg/mL. The inhibition of lipid peroxidation in porcine (*Sus scrofa*) brain cell homogenates was assessed spectrophotometriclly by measuring the reduction in TBARS and the color intensity of malondialdehyde–thiobarbituric acid (MDA–TBA) using absorbance readings at 532 nm.

The lipid peroxidation inhibition ratio (%) was calculated using the following formula:

$$(A - B)/A \times 100$$

where A and B represent the absorbance values of the control and extract samples, respectively. The results were expressed as EC_{50} values (μg/mL), indicating the extract concentration providing 50% antioxidant activity. A positive control was employed, using Trolox (Sigma-Aldrich, St. Louis, MO, USA). The results were presented as the extract concentration achieving 50% inhibition (EC_{50}), obtained from the graph depicting the percentage inhibition against the extract concentration.

Results and discussion

Structure and anatomy

The external appearance of the bark of *Q. vulcanica* is grey and fissured (Fig. 1A). The bark tissues, namely rhytidome and phloem, were macroscopically distinct in the transverse sections (Fig. 1B). Sequential periderms, abundant sclerified tissue, and fused rays were also distinct, while the growth rings were apparent. The bark thickness was approximately 1.2 cm. The external appearance of *Q. vulcanica* bark (Fig. 1A) is consistent with that of most *Quercus* species. The bark thickness was similar to that of *Q. rotundifolia* (1.2 cm) (Sousa et al. 2021) and *Q. faginea* (1.0 cm) (Quilhó et al. 2013), wider than that of *Q. dentata*, *Q. mongolica* and *Q.serrata* (0.5–0.6 cm) (Furuno 1990), but thinner than the barks of *Q. robur* (9 cm) (Trockenbrodt 1994) and *Q. cerris* (3–7 cm) (Şen et al. 2011).

The bark microscopic structure is illustrated in Figs. 2, 3, 4, 5 for transverse and longitudinal sections, in Fig. 6 for the dissociated cells, and in Fig. 7 for the SEM observations. The rhytidome (Fig. 2A–C) is persistent and enclosed the innermost periderm and three subsequent periderm layers, which are separated by layers of non-conducting phloem. The phloem showed a regular and organized structure, with stratified tangential bands of fibres, nodules of sclereids, and broad phloem rays (Fig. 2C).

The periderm (Figs. 3A, B, 5, 7A) was poorly developed, somewhat undulating and anastomosed, with a small proportion of cork (phellem cells, Fig. 6A). The phellem was composed of 3–6 layers of cells sometimes radially flattened, with uniform lignified thickenings in the tangential and radial walls. The cell often contained dark contents, presumably phenolic compounds. The phelloderm in each periderm consisted of 1–3 rows of rectangular to round cells with thin walls and aligned radially.

The phloem of *Q. vulcanica* consisted of conducting phloem, which was a narrow band near the vascular cambium, followed by the non-conducting phloem. In transverse view, the phloem of *Q, vulcanica* was layered regularly from the

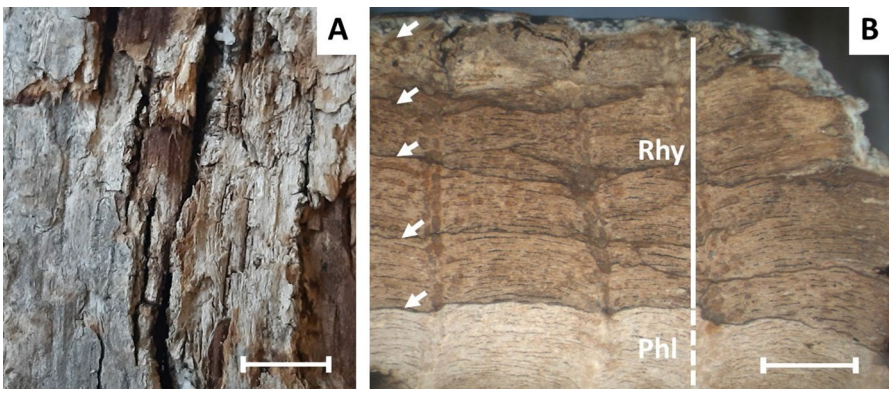

Fig. 1 Bark structure of *Quercus vulcanica* on the transverse section. **A**: General aspects of rhytidome. **B**: Phloem (Phl), rhytidome (Rhy) and sequential periderms (arrows). Scale bar: $A = 1$ cm; $B = 2$ mm

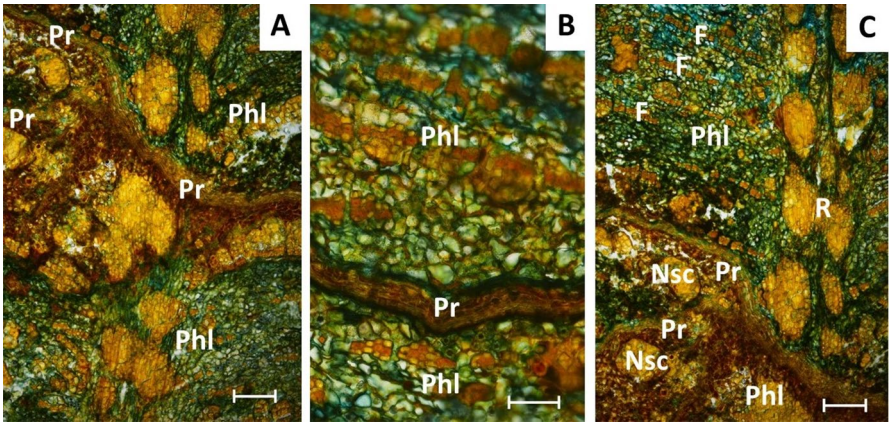

Fig. 2 Transverse view of the rhytidome of *Quercus vulcanica*. **A**, **B**: Periderm (Pr); phloem (Phl). **C**: Periderm (Pr); phloem (Phl) exhibiting tangential bands of fibers (F), broad ray (R) with sclereid nodules (Nsc). Scale bar *A* & *C* = 200 µm; *B* = 100 µm

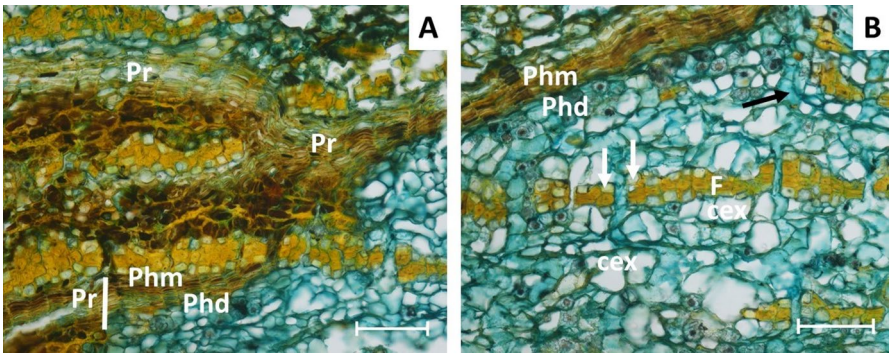

Fig. 3 Transverse view of *Quercus vulcanica* bark. **A**: Periderm (Pr) (_) undulating and anastomosed with phellem (Phm) and phelloderm (Phd) cells. **B**: phellem (Phm) and phelloderm (Phd) and a portion of outer phloem showing dilatation tissue i.e. expanded parenchyma cells (cex), and distortion and dilatation of ray cell (black arrow); crystals (white arrows) bordered the tangential band of fibres (F). Scale bar *A* & *B* = 100 µm

vascular cambium towards the periphery, even in the non-conducting phloem, where the structure was unaltered. Tangential layers of thin walled axial parenchyma cells (storage tissue) and sieve tube elements with companion cells (conducting tissues) alternate with tangential bands of thick-walled fibres and sclereids. The sclereids formed conspicuous nodules (mechanical support tissues) with embedded large prismatic crystals. Thin and large rays crossed the tangential bands of tissues (Fig. 4A).

The sieve tube elements were solitary or in groups of 2 or 3 cells with a round to an irregular shape in transverse section, with 1–2 companion cells, interspersed with strands of parenchyma cells. The sieve plates exhibited a scalariform type,

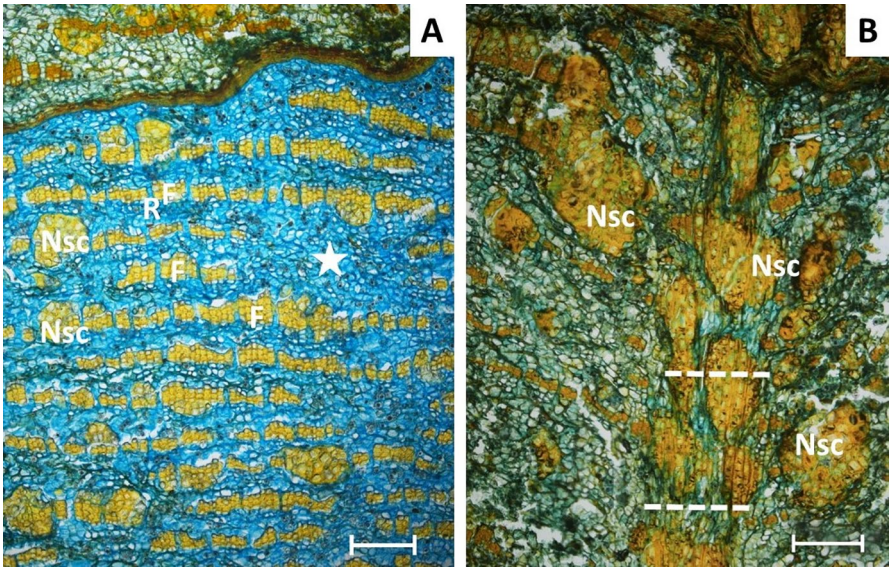

Fig. 4 Secondary phloem of *Quercus vulcanica* in the transverse view. **A**: The tangential bands of fibres (F) interrupted by the nodules of sclereids (Nsc) and axial parenchyma scattered with sieve elements (asterisk). **B**: Sclerified parts of this multiseriate rays (---) and accompanying nodules of sclereids (Nsc). Scale bar *A* & *B* = 200 µm

with 5–6 sieve areas and numerous sieve pores (Figs. 5, 7D); lateral sieve areas were also well-developed (Figs. 5, 7C).

The axial parenchyma was arranged in tangential strands of 2–4 thin-walled cells with a round to rectangular shape in transverse section. These stands were placed between the tangential bands of fibres and scattered with sieve elements, which were hard to distinguish from the axial parenchyma cells. In both transverse and longitudinal sections, strands of crystal-bearing axial parenchyma of approximately equal length (6 to > 10 cells) were observed along the margins of fibre bands (Figs. 3B, 5A, B, 6B, 7B). In the outer non-conducting phloem, particularly near the periderm, the axial parenchyma cells were expanded (Fig. 3B).

The phloem rays, which make up the outward continuation of the wood rays, were homocellular and comprised of procumbent cells (Fig. 5 A). Two sizes were observed: narrow uniseriate rays (Figs. 4A, 5B) and broad rays (multiseriate, up to 20 cells wide and > 100 cells high), (Fig. 4B). The narrow uniseriate rays followed a straight to undulated direction in the beginning of the conducting secondary phloem with minimal dilatation (Fig. 3B), due to the tangential stretching and anticlinal cell divisions; in the broad multiseriate rays, the sclerification started early near the cambium (Fig. 4B) and the sclerified parts of the rays and accompanying groups of sclereids appeared with a palm-like arrangement.

The sclerenchyma tissue consists of fibers and sclereids. Fibres (Fig. 6B) are slender with thick walls, tapered overlapping ends, and arranged in continuous tangential bands of 3–5 cells (Fig. 4A). These bands are often interrupted by clusters of sclereids (Fig. 4A). Sclereids were mostly isodiametric in shape, varying in size,

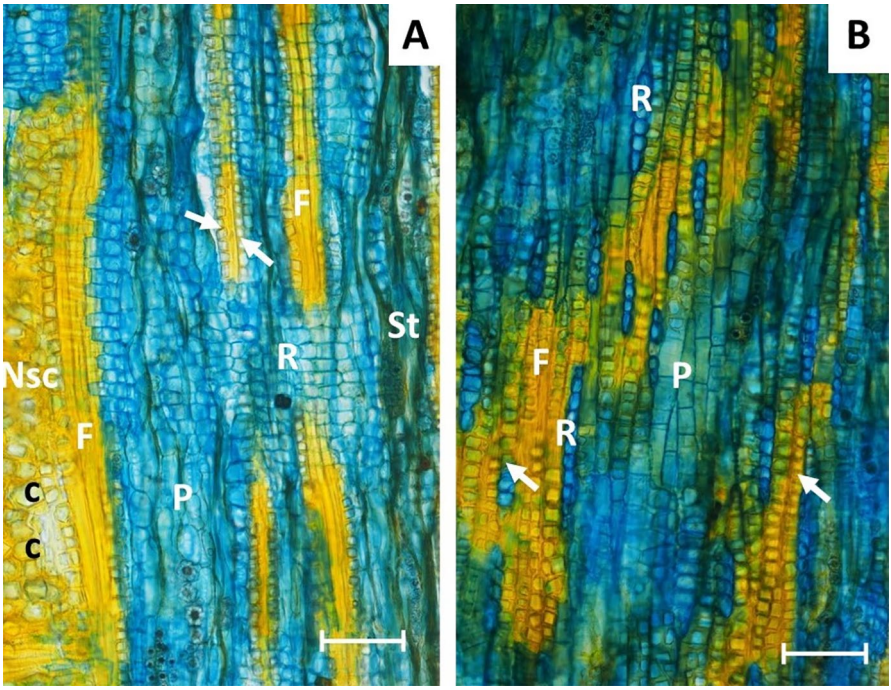

Fig. 5 Secondary phloem of *Quercus vulcanica* in longitudinal view. **A**: Large nodules of sclereids (Nsc) are present, along with crystals (c); homocelular rays (R); fibres (F) bordered by crystalliferous axial parenchyma (crystals, arrow), axial parenchyma (P) and sieve tubes (St) (radial view). **B**: Uniseriate rays (R); fibres (F) bordered by crystalliferous axial parenchyma (arrow), and axial parenchyma (P). Scale bar *A* & *B* = 200 µm

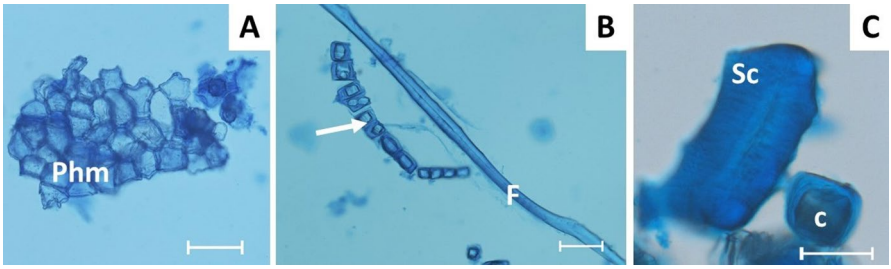

Fig. 6 Individualized cells of *Quercus vulcanica* bark. **A**: Phellem cells (Phm). **B**: Fibre (F) crystalliferous parenchyma cells (arrow); sclereid (Sc) and crystal (**C**). Scale bar *A* & *B* = 50 µm; C = 25 µm

and possessed thick concentrically stratified walls along with numerous pit canals (Fig. 6C). Prominent nodules of sclereids with radial or tangential arrangement occurred within and near the broad rays (Fig. 4B).

The phloem structure in *Q. vulcanica* is similar to that of other *Quercus* species, such as *Q. velutina*, *Q. rubra*, *Q. alba*, and *Q. coccinia* (Howard 1977), *Q.*

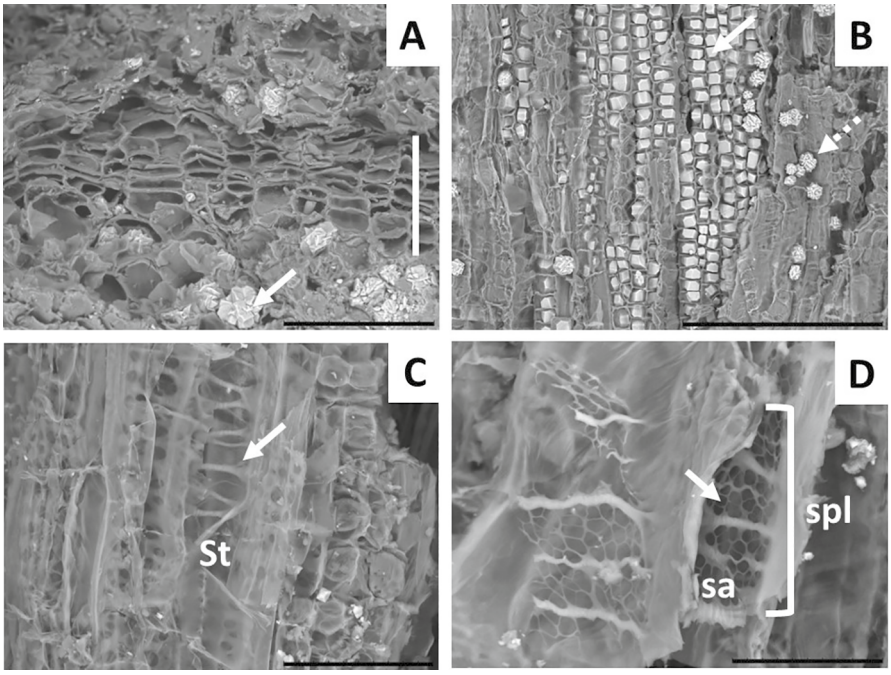

Fig. 7 Scanning electron microscopy of *Quercus vulcanica* bark. **A**: Periderm (Pr) (_); druses (arrow). **B**: Crystalliferous parenchyma cells (prismatic crystals, arrow) and druses (dashed arrow); **C**: sieve tubes with lateral sieve areas (arrow); **D**: sieve plate (spl) with sieve areas (sa) and pores (arrow). Scale bar $A = 100$ µm, $B = 200$ µm, $C = 50$ µm, $D = 30$ µm

robur (Whitmore 1963; Trockenbrodt 1991), *Q. cerris* (Şen et al. 2011), *Q. faginea* (Quilhó et al. 2013), *Q. petraea* (Gričar et al. 2015), and *Q. rotundifolia* (Sousa et al. 2021), as well as cork-rich species like *Q. suber* (Pereira 2007) and *Q. variabilis* (Ferreira et al. 2016). The main features include a regular layered phloem from the cambium to the last formed periderm in successive tangential bands of fibres and groups of sclereids alternated with axial parenchyma and sieve tubes, with conspicuous nodules of cluster sclereids with radial and tangential alignment (Fig. 4) and prominent crystalliferous parenchyma cells (Figs. 5A, B, 6B, 7B).

The rhytidome is comparatively thin (Fig. 1B) containing narrow periderms with a phellem with only a few radial rows of cork cells of small radial dimension (Fig. 2A, 3A, B, 5A, 7A). This differs from other oaks that have cork-rich rhytidomes, where the cork layers are substantial, such as *Q. cerris* (Şen et al. 2011), or in oaks with a single periderm with thick cork, like *Q. suber* (Pereira 2007) and *Q. variabilis* (Ferreira et al. 2016).

The inorganic contents of the bark included druses (Figs. 5A, 7A) and prismatic crystals, presumably of calcium oxalate. These crystals were abundant in the axial chambered parenchyma cells (Fig. 5A, B, 6B, 7B) as well as in the nodules of sclereids (Fig. 7A). The presumably phenolic compounds were observed in various parts of the bark, such as phellem cells, axial and radial parenchyma, and sclereids in the phloem and rhytidome (Figs. 2A–C, 3A).

Chemical composition

The overall chemical composition of *Q. vulcanica* bark is presented in Table 1. The bark includes a significant quantity of inorganic compounds (16.4%) and extractives (23.1%), predominantly comprising hydrophilic compounds soluble in EtOH and H_2O, accounting for 87% of all extractives. The suberin content is low (3.7%) and the lignin content is moderate at 22%.

The monomeric composition of *Q. vulcanica* polysaccharides is displayed in Table 1. Bark polysaccharides consist primarily of glucose and xylose monomers, with smaller quantities of arabinose, galactose, and rhamnose sugars. The hydrolysate also contains acetyl groups, which are characteristic markers of hardwood bark and wood hemicelluloses (Fengel and Wegener 1984).

The only study found on *Q. vulcanica* bark pertains to certain aspects of its chemical composition, including the content of structural components and polyphenols, as well as the composition of cyclohexane extractives and monosaccharides (Balaban and Uçar 2001). The results of that study revealed that *Q. vulcanica* bark contains approximately 13.5% ash, 25.9% extractives, and 10.6% polyphenols, while the lignin and holocellulose contents exhibited a high variability and the cyclohexane extractives were fractionated into saponifiables and neutrals.

The extractive and ash yields of our study (16.4% and 23.1% respectively) are consistent with the findings of that study (Balaban and Uçar 2001). The high ash content of the bark is corroborated by the anatomical observations, which revealed the presence of numerous crystals in the parenchyma cells bordering the fibres (Figs. 5A, B, 6B, 7B).

Table 1 Chemical composition (in % of o.d weight) of *Quercus vulcanica* bark

Summative chemical composition	% of dry mass
Ash	16.4 ± 0.9
Extractives	23.07 ± 2.07
DCM	2.7 ± 0.2
EtOH	10.29 ± 0.99
H_2O	10.09 ± 0.89
Suberin	3.70 ± 0.26
Lignin	21.88 ± 0.38
Klason lignin	18.84 ± 0.32
Acid-soluble lignin	3.04 ± 0.07
Polysaccharide/Lignin ratio	1.60
Polysaccharides composition	
Glucose	14.41
Rhamnose	0.22
Arabinose	1.41
Galactose	1.02
Xylose	7.88
Acetyl groups	0.31

The major extractive fraction consisted of hydrophilic extractives (ethanol and water soluble extracts), which accounted for approximately 88% of the total extractive content (Table 1). The suberin content of *Q. vulcanica* bark was low (3.7%) which is in agreement with the anatomical characterization indicating a low amount of cork in the periderms (Fig. 3). The lignin content was 21.9% (or 26.2% on an ash-free basis), which is lower than the average values found in barks (40–50% on an ash-free basis). However, the polysaccharide content (41.8% on an ash-free basis) fell within the average values observed in different barks (Harkin and Rowe 1971).

Q. vulcanica bark polysaccharides are primarily composed of glucose and xylose monomers (Table 1) which is in agreement with the polysaccharide composition of hardwoods and hardwood barks, namely regarding the xylan predominance in hemicelluloses (Fengel and Wegener 1984). Additionally, *Q. vulcanica* bark contains small amounts of other hemicellulose monomers such as arabinose, galactose, and rhamnose, as well as acetyl groups. This monomeric composition of polysaccharides is similar to previous reports on *Q. vulcanica* bark and wood (Ucar et al. 1999). The polysaccharide to lignin ratio (PLR) of *Q. vulcanica* bark is 1.60, which was lower than the 0.86 observed in *Q. cerris* phloem (Şen et al. 2010). The lignin composition is likely to be a G-rich lignin as suggested by FTIR results (Faix and Beinhoff 1988).

Inorganic elemental composition

The elemental inorganic composition of *Q. vulcanica* bark is presented in Table 2, both as the bark content and the proportion of all the inorganic elements. It is primarily composed of calcium, accounting for 96.5% of the total elements with also the presence of potassium (1.8%), magnesium (0.4%), phosphorus (0.3%), sodium (0.2%) and manganese (0.2%). The bark also contains oligoelements such as iron, copper, and zinc, as well as sulfur (0.5%).

The inorganic composition of *Q. vulcanica* bark is reported for the first time in this study (Table 2). The calcium content falls within the maximum range reported for barks (97%) (Fengel and Wegener 1984). The FTIR spectrum of *Q. vulcanica*

Table 2 Elemental composition of *Quercus vulcanica* bark

Element	mg kg^{-1}	%
Na	113.89	0.21
K	1029.11	1.85
Ca	53,565.21	96.5
Mg	229.58	0.41
P	139.23	0.25
S	281.80	0.51
Fe	38.01	0.07
Cu	7.99	0.01
Zn	2.22	0.00
Mn	103.21	0.19
Total	55,510.26	100

bark confirms the presence of calcium oxalate, indicated by the peaks at 512 cm^{-1}, 781 cm^{-1}, 1316 cm^{-1}, and 1618 cm^{-1}. The presence of calcium-oxalate crystals was also reported in other barks such as *Quercus robur*, *Ulmus glabra*, *Betula pendula*, and *Populus tremula* (Trockenbrodt 1995). The anatomical characterization confirms the abundant presence of crystals in parenchyma cells (Fig. 5A, B). The sulfur content of the bark was relatively high, which may be related to the soil composition of the sampling site, as the area contains sulfur reserves according to the Mineral Research and Exploration Institute (MTA) of Turkey.

FTIR analysis

The FTIR spectrum of *Q. vulcanica* bark is depicted in Fig. 8, and the assignment of the main peaks to chemical components is provided in Table 3. The spectrum is dominated by peaks at 779 cm^{-1}, 1316 cm^{-1}, and 1611 cm^{-1} that are assigned to C–O and C=O stretching vibrations of calcium oxalate (Pinzari et al. 2010). The broad band at 3332 cm^{-1} is attributed to O–H stretching. The band with maxima between 2920 and 2921 cm^{-1} and the less resolved and small band at 2852 cm^{-1} are assigned to C–H stretching vibrations of methylene groups in suberin (Sen et al. 2023). The two bands with maxima at 1714–1720 cm^{-1} and 1726–1727 cm^{-1} are assigned to carbonyl groups (C=O) of ester structures of unsaturated and saturated fatty acids and suberin monomers (Sen et al. 2023).

The conspicuous band at 1031 cm^{-1} is associated with overlapping C–O vibrations of polysaccharides and C–H deformations of guaiacyl lignin (Faix and Beinhoff 1988). The presence of guaiacyl lignin is an interesting feature of *Q. vulcanica* bark because the IR spectrum also contains other specific markers of guaiacyl lignin such as the bands at 1143 cm^{-1} (C–H deformation in guaiacyl ring) (Faix and Beinhoff 1988), and at 1262 cm^{-1} (guaiacyl ring breathing) (Yan

Fig. 8 FTIR spectrum of *Quercus vulcanica* bark

Table 3 Peak assignment in FTIR spectrum of *Quercus vulcanica* bark

Signal (cm^{-1})	Functional group	Assignment to chemical components	Reference
779	O–C–O	CaOxa	Pinzari et al. (2010)
1031	C–O in polysaccharides and C–H in guaiacyl ring	Cellulose/lignin	Faix and Beinhoff (1988)
1143	C–H in guaiacly ring	Lignin	Faix and Beinhoff (1988)
1262	Guaiacyl ring breathing	Lignin	Yan et al. (2016)
1316	O–C–O	CaOxa	Pinzari et al. (2010)
1370	C–H	Polysaccharides	Traoré et al. (2016)
1514	C=C	Lignin	Kubo and Kadla (2005)
1611	C=O	CaOxa	Pinzari et al. (2010)
2921	C–H	Suberin	Sen et al. (2023)
3345	O–H	Moisture or phenolic structures	Sen et al. (2023)

et al. 2016). The small band at 1370 cm^{-1} is assigned to C–H deformations in cellulose and hemicelluloses (Traoré et al. 2016), while the other small band was observed at 1514 cm^{-1} assigned to the C=C aromatic skeletal stretching vibrations of the benzene ring in lignin (Kubo and Kadla 2005).

Composition of lipophilic extractives

The lipophilic composition of *Q. vulcanica* bark comprises mainly terpenoids, accounting for 72.2% of the total, with friedelin and friedelin derivatives as the major compounds with minor triterpenoids including betulinic acid and ursolic acid (Table 4). Steroids, particularly β-sitosterol, are also present as important constituents. These results regarding the lipophilic composition align with previous findings, where significant amounts of friedelin and sitosterol were identified in the neutral fraction of *Q. vulcanica* bark (Balaban and Uçar 2001). The lipophilic composition of *Q. vulcanica* bark is similar to that of cork-rich barks such as *Q. cerris* and *Q. suber* (Pereira 2007; Şen et al. 2015), despite the fact that *Q. vulcanica* bark does not contain a significant amount of cork. Oak barks in general appear to be abundant sources of triterpenoids, and friedelin, in particular, is an interesting compound known for its bioactive properties, including anti-inflammatory and anti-tumor effects (Lu et al. 2010; Antonisamy et al. 2011). Previous studies reported high yields of friedelin extraction from *Q. cerris* bark using supercritical CO_2 extraction (de Melo et al. 2020). Therefore, despite *Q. vulcanica* bark yielding a low amount of lipophilic extractives (2.7%) through solvent extraction, the utilization of enhanced extraction methods may increase the yield, thereby allowing considering them in a biorefinery integrated flowsheet.

Table 4 Composition of the lipophilic extractives (dichloromethane solubles) of *Quercus vulcanica* bark

Compound families	Compounds	% of total peak area
Alcohols	Total	1.43
	Hexadecanol	0.08
	Octadecanol	0.09
	Eicosanol	0.22
	Docosanol	0.35
	Tetracosanol	0.46
	Hexacosanol	0.08
	Octacosanol	0.15
Fatty acids	Total	7.48
	Tetradecanoic acid	0.24
	Pentadecanoic acid	0.12
	Hexadecanoic acid	2.91
	Heptadecanoic acid	0.09
	9,12-Ocatdecadienoic acid	0.44
	9-Octadecenoic acid	0.61
	Octadecanoic acid	0.62
	Eicosanoic acid	0.21
	Heneicosanoic acid	0.35
	Docosanoic acid	0.51
	Tetracosanoic acid	0.64
	Pentacosanoic acid	0.05
	Hexacosanoic acid	0.69
ω-hydroxy fatty acids	Total	0.78
	22-Hydroxydocosanoic acid (2TMS)	0.62
	24-Hydroxytetracosanoic acid (2TMS)	0.16
Phenolics	Total	2.18
	Benzoic acid	0.08
	Vanillin	0.08
	Ferulic acid	0.04
	Tetracosyl ferulate	0.33
	Hexacosyl (E)-ferulate	1.23
	Octacosyl (E)-ferulate	0.42
Steroids	Total	11.24
	Stigmasterol	0.13
	β-sitosterol	9.31
	Stigmastanol	1.08
	Stigmast-4-en-3-one	0.73

Table 4 (continued)

Compound families	Compounds	% of total peak area
Terpenoids	Total	72.19
	β-Amyrone	0.47
	Lupeol	1.06
	Friedelan-2-one	36.64
	Friedelanol	26.19
	Oleanolic acid	2.25
	Betulinic acid	3.11
	Ursolic acid	2.47
Sugars	Total	1.04
	Sitosteryl-3β-D-Glucopiranoside	1.04
Gylcerol derivatives	Total	2.38
	Glycerol	2.07
	Tetracosyl glycerol	0.32

Suberin composition

The composition of suberin, categorized by chemical families, in *Q. vulcanica* bark is presented in Table 5. It is expressed as mass percent of the bark and as a proportion of the total monomers. Suberin comprises lipid monomers that are soluble in dichloromethane, as well as water-soluble glycerol that was quantified in the aqueous fraction of the methanolysis reaction. The major chemical families include α, ω-diacids and ω-hydroxyacids which together accounted for about 69.0% of all monomers released (equivalent to 2.5% of the bark). Glycerol accounts for 4.9% of all released monomers (equivalent to 0.18% of bark).

The monomeric composition of suberin, based on peak areas of GC–MS chromatograms of the organic phase of the acidified methanolysates, is reported in Table 6.

Table 5 Suberin composition (in % of bark and in % of total monomers) including glycerol, long chain aliphatic compounds and aromatics solubilized by methanolysis of the bark of *Quercus vulcanica*

Chemical family	% of bark	% of monomers
Glycerol	0.18	4.90
Alkanoic acids	0.53	14.23
ω-Hydroxyalkanoic acids	1.24	33.56
α, ω-Alkanoic diacids	1.31	35.43
Alkanols	0.26	7.11
Glycerol derivatives	0.04	1.15
Aromatic compounds	0.04	1.13
Total	3.70	

Table 6 Suberin monomeric composition of *Quercus vulcanica* bark expressed in % of the chromatographic peak areas

Compound families	Compounds	% of total peak area
Alcohols	Total	7.11
	Octadecanol	0.31
	Eicosanol	0.06
	Docosanol	3.77
	Pentadecanol	0.53
	1,22-Docosanediol	0.33
	Octacosanol	1.36
	Hexacosanol	0.75
Fatty acids	Total	14.23
	Hexadecanoic acid, methyl ester	0.44
	Hexadecanoic acid, TMS	0.32
	9- Octadecenoic acid, methyl ester (Z)	0.31
	Octadecanoic acid, methyl ester	0.11
	Octadecanoic, acid, TMS	1.84
	Docosanoic acid, methyl ester	3.70
	Tridecanoic acid, TMS	1.29
	Metil 2-hydroxytetradecanoate, TMS	1.55
	Tetracosanoic acid, methyl ester	2.29
	Docosanoic acid, TMS	
	Hexacosanoic acid, methyl ester	0.79
	15-Tetracosenoic acid, TMS	1.61
α-ω-dicarboxylic acids	Total	35.43
	Hexadecanedioic acid, dimethyl ester, C16:0, dimetil ester	12.47
	Octadec-9-enedioic acid, dimetil ester	20.57
	Octadecanedioic acid, dimetil ester	0.77
	Eicosanedioic acid, dimetil ester	0.47
	Docosanedioic acid, dimetil ester	0.55
	Octadecanedioic acid 9,10-dihydroxy(di-TMS)-dimethyl ester, threo	0.26
	Octadecanedioic acid 9,10-dihydroxy(di-TMS), 1,18-(dimethylsilyl)	0.33
ω-hydroxy acids	Total	33.56
	Hexadecanoic acid, (16-trimetilsiloxy)-, methyl ester	5.37
	Methyl 18-hydroxy-9-octadecenoate, TMS derivative	26.10
	Docosanoic acid, (22-trimethylsiloxy)-, methyl ester	1.83
	Tetracosanoic acid, (24-trimethylsiloxy)-, methyl ester	0.26
	Hexacosanoic acid, (26--trimethylsiloxy)-, methyl ester	5.37
Phenolics	Total	1.13
	Vanillin	0.19
	methyl isoferulate, TMS	0.22
	methyl ferulate, TMS	0.72

Table 6 (continued)

Compound families	Compounds	% of total peak area
Glycerol derivatives	Total	1.87
	2-oleoglycerol, 2 TMS (9-Octadecenoic acid, 1,3-bis-(O-TMS)-2-Propyl ester	1.15
	docosyl glycerol (C22:0)	0.72

It includes the long-chain aliphatic compounds and aromatics that were soluble in the organic phase, and therefore does not include the glycerol that is reported in Table 6 separately. The major components are α, ω-diacids, accounting for 35.4% of the total monomers (14.3% saturated α, ω-diacids, and 21.2% unsaturated and substituted α, ω-diacids) and by ω-hydroxyacids, representing 33.6% of the total monomers (7.5% saturated hydroxyacids and 26.1% substituted hydroxyacids). Alkanoic acids make up 14.2% of the monomers, while alkanols account for 7.1%. In smaller amounts, glycerides derivatives (1.9%) and aromatics (1.1%) were also identified. The main individual monomers of *Q. vulcanica* bark suberin were 18-hydroxy-9-octadecenoic acid (26%) and octadec-9-enedioic acid (20.6%), with hexadecanedioic acid (12.5%), docosanoic acid (3.7%), hexadecanoic acid (5.4%), and hexacosanoic acid (5.4%) also being important monomers.

The main long chain monomers of *Q. vulcanica* bark suberin were α, ω-carboxylic diacids and ω-hydroxy acids in similar amounts, with 18-hydroxy-9-octadecenoic acid and octadec-9-enedioic acid as the principal monomers (Table 6). The monomer composition of suberins is highly variable between species. For instance, ω-hydroxy acids content of *Q. vulcanica* is smaller than that of *Q. suber* (up to 48%) (Bento et al. 2001) and *Q. cerris* (up to 90%) (Şen et al. 2010). This variability in suberin composition even occurs in the same species, and a higher variability was observed in *Q. suber* virgin cork compared to reproduction cork (Bento et al. 2001). The presence of dicarboxylic acid monomers is a distinctive feature of suberin, which differentiates it from cutin, another important plant bioester (Pollard et al. 2008). For instance, the cutin in *Q. suber* leaves is mainly composed of ω-hydroxyacids, followed by fatty acids, with only a few α, ω–diacids (Simões et al. 2021). Ferulic acid derivatives are the main phenolic components of *Q. vulcanica* suberin, similar to *Q. suber* and *Q. cerris* corks (García-Vallejo et al. 1997; Şen et al. 2010).

Antioxidant activity of hydroethanolic extracts

The results of the antioxidant properties of the hydroethanolic extracts of *Q. vulcanica* bark are presented in Table 7. The extract yield was 10.2% and its antioxidant activity was high, with an EC_{50} value of 55 µg/mL.

The hydroethanolic extracts exhibited a surprisingly high antioxidant activity, as determined by the TBARS method (Table 7). The extract yield was high under the mild conditions used (10.2%) but there is scope to enhance the yield, given the total

Table 7 Ex-vivo antioxidant properties of *Quercus vulcanica* bark

Extract yield (%)	10.2
TBARS ($EC_{50,}$ µg/mL)	55 ± 1
Trolox (µg/mL)	5.4 ± 0.3

20.4% of ethanol and water solubles present in the bark (Table 1). Therefore, extraction is a key conversion step in the valorization of *Q. vulcanica* bark.

Conclusion

The detailed anatomical properties and chemical composition of the endemic *Q. vulcanica* bark in Turkey were reported here for the first time and discussed from the perspective of integration into a bark-based biorefinery system. The overall results suggest that certain constituents, such as calcium oxalate, polar extractives, C_{18} dicarboxylic acids, friedelin, and ferulic acid, serve as markers for oak barks. Therefore, biorefinery studies for oak barks should focus on the valorization of these compounds. The lignin and polysaccharide contents of *Q. vulcanica* bark were found to be low to average. Considering the high ash content of the bark, thermal conversion may not be a favorable unit operation in biorefineries. Similarly, the low suberin content does not advise a cork-targeted valorization. The distinguishing feature of *Q. vulcanica* bark is its high content of hydrophilic extractives and their strong antioxidant activity, which indicates a promising potential for biorefineries. *Q. vulcanica* bark also yields a low amount of lipophilic extractives. The utilization of enhanced extraction methods may further increase the yield of lipophilic extracts. Therefore, exploring extraction as the initial conversion step offers an advantageous option.

The following specific conclusions can be drawn from this study:

1. The ash content of the bark is high (16.4%), primarily comprising calcium oxalate crystals as confirmed by FTIR analysis.
2. The content of extractives is very high (23.1%), predominantly composed of hydrophilic extractives.
3. Hydroethanolic extracts obtained under mild conditions exhibit antioxidant activity.
4. Lipophilic extractives consist mostly of terpenoids, with friedelin and friedelanol as the main compounds.
5. The suberin content is low, characterized by the presence of α, ω-alkanoic diacids and ω-hydroxyalkanoic acids in similar proportions.

Acknowledgements The authors thank Joaquina Silva from Instituto Superior de Agronomia for chemical analysis, José Condeço and Marta Martins from Instituto Superior Técnico for FT-IR analysis.

Author contributions Conceptualization, US and HP; methodology, US and HP; investigation, US, RS, CY, TQ, VS, AF, and IM; resources, CY; data curation, US and HP; writing—original draft preparation,

US, TQ, and VS; writing—review and editing, US, CY, TQ, IM, AF, and HP; visualization, HP; supervision, HP. All authors have read and agreed to the published version of the manuscript.

Funding This work has been supported by FCT—Fundação para a Ciência e Tecnologia within the R&D Unit Forest Research Centre, CEF (UIDB/00239/2020) and also from the FCT/MCTES (PIDDAC) national funds to CIMO (UIDB/00690/2020 and UIDP/ 00690/2020) and SusTEC (LA/P/0007/2021). U. Sen and V. Sousa acknowledge support from FCT through research contracts (DL 57/2016), R. Simões by a Ph.D. scholarship (PD/BD/128259/2016), and for the national funding by FCT and P.I. in the form of the institutional scientific employment program for the contract of Â. Fernandes.

Data availability Not applicable.

Declarations

Conflict of interest The authors have no relevant financial or non-financial interests to disclose.

References

Angyalossy V, Pace MR, Evert RF et al (2016) IAWA list of microscopic bark features. IAWA J 37:517–615. https://doi.org/10.1163/22941932-20160151

Antoniou N, Monlau F, Sambusiti C et al (2019) Contribution to circular economy options of mixed agricultural wastes management: coupling anaerobic digestion with gasification for enhanced energy and material recovery. J Clean Prod 209:505–514. https://doi.org/10.1016/j.jclepro.2018.10.055

Antonisamy P, Duraipandiyan V, Ignacimuthu S (2011) Anti-inflammatory, analgesic and antipyretic effects of friedelin isolated from Azima tetracantha Lam. in mouse and rat models. J Pharm Pharmacol 63:1070–1077. https://doi.org/10.1111/j.2042-7158.2011.01300.x

Aslan EG, Ayvaz Y (2009) Diversity of Alticinae (Coleoptera, Chrysomelidae) in Kasnak oak forest nature reserve, Isparta, Turkey. Turkish J Zool 33:251–262. https://doi.org/10.3906/zoo-0806-2

Atalay I, Efe R, Öztürk M (2014) Ecology and classification of forests in Turkey. Procedia Social Behav Sci 120:788–805. https://doi.org/10.1016/j.sbspro.2014.02.163

Awasthi MK, Sarsaiya S, Patel A et al (2020) Refining biomass residues for sustainable energy and bioproducts: An assessment of technology, its importance, and strategic applications in circular bioeconomy. Renew Sustain Energy Rev 127:109876. https://doi.org/10.1016/j.rser.2020.109876

Balaban M, Uçar G (2001) Extractives and structural components in wood and bark of endemic oak Quercus vulcanica Boiss. Holzforschung 55:478–486. https://doi.org/10.1515/HF.2001.079

Bento MFS, Pereira H, Cunha MÁ et al (2001) A study of variability of suberin composition in cork from *Quercus suber* L. using thermally assisted transmethylation GC–MS. J Anal Appl Pyrolysis 57:45–55. https://doi.org/10.1016/S0165-2370(00)00093-0

de Melo MMR, Vieira PG, Şen A et al (2020) Optimization of the supercritical fluid extraction of Quercus cerris cork towards extraction yield and selectivity to friedelin. Sep Purif Technol 238:116395. https://doi.org/10.1016/j.seppur.2019.116395

Faix O, Beinhoff O (1988) FTIR spectra of milled wood lignins and lignin polymer models (DHP's) with enhanced resolution obtained by deconvolution. J Wood Chem Technol 8:505–522

Fengel D, Wegener G (1984) Wood: chemistry, ultrastructure reactions. Walter de Gruyter, Berlin

Ferreira J, Miranda I, Şen U, Pereira H (2016) Chemical and cellular features of virgin and reproduction cork from *Quercus variabilis*. Ind Crops Prod 94:638–648. https://doi.org/10.1016/j.indcrop.2016.09.038

Furuno T (1990) Bark structure of deciduous broad-leaved trees grown in the San'in region, Japan. IAWA J 11:239–254. https://doi.org/10.1163/22941932-90001181

García-Vallejo MC, Conde E, Cadahía E, De Simón BF (1997) Suberin composition of reproduction cork from *Quercus suber*. Holzforschung 51:219–224. https://doi.org/10.1515/hfsg.1997.51.3.219

Göker Y, As N, Ünsal Ö (2001) Some technological properties of Quercus vulcanica (Boiss. and Heldr.) Kotschy. J Fac for Istanbul Univ 51:33–42

Gričar J, Jagodic Š, Prislan P (2015) Structure and subsequent seasonal changes in the bark of sessile oak (Quercus petraea). Trees 29:747–757. https://doi.org/10.1007/s00468-015-1153-z

Harkin JM, Rowe JW (1971) Bark and its possible uses. U.S. Department of Agriculture, Forest Service and Forest Product Laboratory FPL-091, Madison, Wisconsin

Howard ET (1977) Bark structure of southern upland oaks. Wood Fiber Sci 9(3):172–183

Kayacık H (1977) Türkiye meşe ormanlarına toplu bir bakış ve bunların geleceği hakkında düşünceler [An overview of oak forests in Turkey and considerations about their future]. J Fac for Istanbul Univ 27:32–40

Kubo S, Kadla JF (2005) Hydrogen bonding in lignin: a Fourier transform infrared model compound study. Biomacromol 6:2815–2821

Lu B, Liu L, Zhen X et al (2010) Anti-tumor activity of triterpenoid-rich extract from bamboo shavings (Caulis bamfusae in Taeniam). African J Biotechnol 9:6430–6436

Merev N (1998) Türkiye meşelerinin (Quercus L.) odun anatomisi [Wood anatomy of Turkish oaks (Quercus L.)]. In: Proceedings of Kasnak Meşesi ve Türkiye Florası Sempozyumu, Istanbul

Pasztory Z, Mohácsiné IR, Gorbacheva G, Börcsök Z (2016) The utilization of tree bark. BioResources 11:7859–7888. https://doi.org/10.15376/biores.11.3

Pereira H (2007) Cork: Biology, Production and Uses. Elsevier, Radarweg 29, PO Box 211. 1000 AE Amsterdam, The Netherlands

Pinzari F, Zotti M, De Mico A, Calvini P (2010) Biodegradation of inorganic components in paper documents: formation of calcium oxalate crystals as a consequence of *Aspergillus terreus* Thom growth. Int Biodeterior Biodegrad 64:499–505. https://doi.org/10.1016/j.ibiod.2010.06.001

Pollard M, Beisson F, Li Y, Ohlrogge JB (2008) Building lipid barriers: biosynthesis of cutin and suberin. Trends Plant Sci 13:236–246. https://doi.org/10.1016/j.tplants.2008.03.003

Quilhó T, Sousa V, Tavares F, Pereira H (2013) Bark anatomy and cell size variation in *Quercus faginea*. Turk J Bot 37:561–570. https://doi.org/10.3906/bot-1201-54

Şen A, Miranda I, Santos S et al (2010) The chemical composition of cork and phloem in the rhytidome of *Quercus cerris* bark. Ind Crops Prod 31:417–422. https://doi.org/10.1016/j.indcrop.2010.01.002

Şen A, Quilhó T, Pereira H (2011) Bark anatomy of *Quercus cerris* L. var. cerris from Turkey. Turk J Bot 35:45–55. https://doi.org/10.3906/bot-1002-33

Şen A, De Melo MMR, Silvestre AJD et al (2015) Prospective pathway for a green and enhanced friedelin production through supercritical fluid extraction of *Quercus cerris* cork. J Supercrit Fluids 97:247–255. https://doi.org/10.1016/j.supflu.2014.12.008

Sen U, Longo A, Gonçalves M et al (2023) The potential of waste phloem fraction of *Quercus cerris* bark in biochar production. Environments 10:71. https://doi.org/10.3390/environments10050071

Simões R, Miranda I, Pereira H (2021) Chemical composition of leaf cutin in six *Quercus suber* provenances. Phytochemistry 181:112570. https://doi.org/10.1016/j.phytochem.2020.112570

Sluiter A, Hames B, Ruiz R et al (2008) Determination of structural carbohydrates and lignin in biomass. Lab Anal Proced 1617:1–16

Sousa V, Ferreira JPA, Miranda I et al (2021) Quercus rotundifolia bark as a source of polar extracts: structural and chemical characterization. Forests 12:1160. https://doi.org/10.3390/f12091160

Traoré M, Kaal J, Cortizas AM (2016) Application of FTIR spectroscopy to the characterization of archeological wood. Spectrochim Acta Part A Mol Biomol Spectrosc 153:63–70. https://doi.org/10.1016/j.saa.2015.07.108

Trockenbrodt M (1991) Qualitative structural changes during bark development in *Quercus robur*, *Ulmus glabra*, *Populus tremula* and *Betula pendula*. IAWA J 12:5–22

Trockenbrodt M (1994) Quantitative changes of some anatomical characters during bark development in *Quercus robur*, *Ulmus glabra*, *Populus tremula* and *Betula pendula*. Iawa J 15:387–398

Trockenbrodt M (1995) Calcium oxalate crystals in the bark of *Quercus robur*, *Ulmus glabra*, *Populus tremula* and *Betula pendula*. Ann Bot 75:281–284

Ucar MB, Yilgor N, Strobel C (1999) Chemical characteristics of endemic oak-wood Quercus vulcanica Boiss. Holz Roh- Werkst 57:152–153

Whitmore TC (1963) Studies in systematic bark morphology: IV. The bark of beech, oak and sweet chestnut. New Phytol 62:161–169. https://doi.org/10.1111/j.1469-8137.1963.tb06323.x

Yaltirik F (1984) Turkiye meseleri teshis klavuzu [Guide for identification of Turkish oaks]. Tarim Orman ve Köyişleri Genel Müdürlüğü, Istanbul

Yan K, Liu F, Chen Q et al (2016) Pyrolysis characteristics and kinetics of lignin derived from enzymatic hydrolysis residue of bamboo pretreated with white-rot fungus. Biotechnol Biofuels 9:1–11

Yücedağ C, Müller M, Gailing O (2021) Morphological and genetic variation in natural populations of *Quercus vulcanica* and *Q. frainetto*. Plant Syst Evol 307:1–15. https://doi.org/10.1007/s00606-020-01737-w

Zieliński J, Petrova A, Tomaszewski D (2006) Quercus trojana subsp. yaltirikii (Fagaceae), a new subspecies from southern Turkey. Willdenowia 36:845–849. https://doi.org/10.3372/wi.36.36214

Authors and Affiliations

Ali Umut Şen[1] · Rita Simões[1] · Cengiz Yücedağ[2] · Teresa Quilhó[1] · Vicelina Sousa[1] · Isabel Miranda[1] · Ângela Fernandes[3,4] · Helena Pereira[1]

✉ Ali Umut Şen
umutsen@isa.ulisboa.pt

[1] TERRA Associate Laboratory, Forest Research Centre (CEF), School of Agriculture (ISA), University of Lisbon, Tapada da Ajuda, 1349-017 Lisbon, Portugal

[2] Department of Landscape Architecture, Faculty of Engineering and Architecture, Burdur Mehmet Akif Ersoy University, Burdur, Turkey

[3] Mountain Research Center, Polytechnic Institute of Bragança, Campus de Santa Apolónia, 5300-253 Bragança, Portugal

[4] Laboratório Associado para a Sustentabilidade e Tecnologia em Regiões de Montanha (SusTEC), Instituto Politécnico de Bragança, Campus de Santa Apolónia, 5300-253 Bragança, Portugal